SENSE and simultaneous multislice imaging

SENSE and Simultaneous Multislice Imaging

Benjamin Zahneisen,[1]* Thomas Ernst,[1] and Benedikt A. Poser[2]

Purpose: Simultaneous multislice (SMS) acquisitions play an important role in the challenge of increasing single-shot imaging speed. We show that sensitivity encoding in two spatial dimensions (two-dimensional sensitivity encoding [2D-SENSE]) can be used to reconstruct SMS acquisitions with periodic but otherwise arbitrary undersampling patterns.

Theory and Methods: By adopting a 3D k-space representation of the SMS sampling process, the accelerated in-plane and slice-encoding directions form a 2D-reconstruction problem that is equivalent to volumetric controlled aliasing in parallel imaging results in higher acceleration (CAIPIRINHA). 2D-SENSE does not otherwise distinguish between standard volumetric and SMS imaging with arbitrary CAIPIRINHA sampling.

Results: Use of the SENSE algorithm is demonstrated for in vivo brain data obtained with blipped-CAIPRINHA sampling in 2D SMS-echo planar imaging (EPI) and rapid acquisition with relaxation enhancement (RARE) acquisitions as well as 3D-EPI with various in-plane and through-plane acceleration factors and CAIPIRINHA shifts. The proposed SENSE reconstruction works for any combination of SMS-factor and CAIPIRINHA shift by the addition of "dummy slices" that allow for noninteger undersampling in the slice direction. Images with commonly used slice-generalized autocalibrating partially parallel acquisitions reconstruction are shown for reference.

Conclusion: SENSE is conceptually simple and provides a one-step reconstruction along both undersampled dimensions. It also provides a contrast-independent parallel imaging reconstruction for SMS. **Magn Reson Med 74:1356–1362, 2015.**

Key words: simultaneous multi slice; SMS; SENSE

INTRODUCTION

Parallel undersampled simultaneous multislice (SMS) imaging (1,2) has recently gained popularity, especially for 2D single-shot sequences such as echo-planar imaging (EPI) for which in-plane parallel imaging only results in marginal reductions of volume repetition time (TR). The initial demonstrations of SMS-EPI (2) use a sensitivity encoding/generalized autocalibrating partially parallel acquisitions (SENSE/GRAPPA) approach to separate the slices (3). Blipped-controlled aliasing in parallel imaging results in higher acceleration (CAIPIRINHA) (2,4) for SMS acquisitions is generally preferred because it reduces g-noise penalty by distributing the aliasing energy more evenly in image space. However, it is incompatible with SENSE/GRAPPA because sharp signal discontinuities arise when concatenating the field of view (FOV)-shifted reference slices to form the SENSE/GRAPPA calibration data. These signal discontinuities can lead to phase errors in the reconstructed image. As a solution, Setsompop has proposed a multikernel GRAPPA method (slice-GRAPPA) for which a separate kernel is fitted for every slice (2). Crucially, with the exception of abstracts by refs (5–7), most SMS reconstructions employ a two-step approach to first disentangle the aliased slices and then perform in-plane parallel reconstruction, or vice versa. Here we propose to use SENSE (8), along two undersampled directions (2D-SENSE (9)), for reconstruction of simultaneously excited slices as a general one-step approach to reconstruct SMS data with arbitrarily undersampled Cartesian k-space in phase and/or slice directions. A SENSE approach is conceptually straightforward, easy to implement, and well understood. Because contrast-independent coil sensitivities from a reference scan are used, a SENSE approach can easily be employed for cases in which the contrast of the target image considerably differs from the reference scan. Furthermore, by using SENSE (or equivalently a one-step, 3D-GRAPPA (5,6)), the same reconstruction algorithm can be used to reconstruct SMS and conventional 3D-imaging with or without CAIPIRINHA k-space patterns. This will facilitate signal-to-noise ratio (SNR) comparisons between SMS and 3D-imaging modalities (e.g., SMS-EPI (2) and 3D-EPI (10–12)) because no algorithm implementation-dependent bias is introduced.

In this work, a SENSE reconstruction is applied to blipped-CAIPI SMS-EPI acquisitions as well as a SMS-rapid acquisition with relaxation enhancement (RARE) sequence using CAIPIRINHA sampling and power independent of number of slices (PINS) excitation (13,14). Furthermore, as an example of 3D-encoding following volumetric slab excitation, we show results from a 3D-EPI acquisition with 2D-undersampling using a CAIPIRINHA pattern.

THEORY

Simultaneous Multislice Imaging and 3D K-Space

The motivation for 2D-SENSE reconstruction becomes obvious when adopting a 3D k-space representation of the SMS sampling process, as described in (5) and (15). The read direction is assumed to be fully sampled; therefore, the two remaining phase encode directions (in-plane and slice direction) form a 2D-reconstruction problem mathematically equivalent to that of volumetric

[1]University of Hawaii, Department of Medicine, John A. Burns School of Medicine, Honolulu, Hawaii, USA.

[2]Maastricht University, Faculty of Psychology and Neuroscience, Department of Cognitive Neuroimaging, Maastricht, The Netherlands.

Grant sponsor: NIH; Grant numbers: 1R01 DA021146 (BRP); U54 56883 (SNRP); and K02-DA16991; Grant sponsor: Brains Unlimited/Scannexus; Grant number: D0069.

*Correspondence to: Benjamin Zahneisen, University of Hawaii JABSOM, The Queen's Medical Center, 1356 Lusitana Street 7th floor, Honolulu, Hawaii 96813, USA. E-mail: benjamin.zahneisen@gmail.com

Received 7 August 2014; revised 16 October 2014; accepted 16 October 2014

DOI 10.1002/mrm.25519

Published online 5 November 2014 in Wiley Online Library (wileyonlinelibrary.com).

CAIPIRINHA (4). In this framework, the reconstruction algorithm does not distinguish between standard volumetric imaging with 3D Fourier encoding and SMS imaging with optimized k-space sampling pattern.

Given an undersampled k-space, the resulting image aliasing pattern is obtained by the Fourier transform of the sampling pattern, with zeros and ones encoding skipped and acquired samples, respectively. The aliasing pattern is the point spread function of a particular undersampling pattern in k-space (see Figures 1a and 1b). The total number of nonzero entries of the aliasing pattern defines the total acceleration factor AF_{tot}. For practical purposes, the aliasing pattern for a single voxel at location $\mathbf{r}_i = (r_{xi}, r_{yi}, r_{zi})$ directly provides the matrix indices of the aliased voxels $\tilde{\mathbf{r}}_{ij}$ with $j = 1 \ldots AF_{tot}$, which have to be separated. This allows for a most general and convenient implementation of the 2D-SENSE algorithm. For a more detailed description of SENSE with arbitrary undersampling patterns along two dimensions, we refer to the literature, especially (9) and (4).

Figure 1a shows an example of four simultaneously excited slices ($AF_z = 4$), factor-2 in-plane undersampling ($AF_{pe} = 2$), and CAIPI-shift 2Δkz. The SENSE-aliasing pattern in Figure 1b has $AF_{tot} = 2 \times 4 = 8$ nonzero entries, whereas the y-axis scales with the image resolution. Typically, the number of slices in an SMS group is on the same order or even smaller than the total acceleration factor. Therefore, the definition of a quadratic sampling cell with length equal to the total acceleration factor as defined in (4) is ambiguous and cannot be readily applied to yield an analytical formulation of the coil sensitivity indices. Because of the periodicity of k-space, it is possible to define dummy slices with zero signal intensity and fill up the sampling cell along the slice direction. However, for the sake of clarity we are using sampling cells (representing k-space undersampling) with the dimension along the slice direction equal to the number of slices in an SMS group.

Noninteger Slice Undersampling

Cartesian SENSE (8) generally is taken to imply a regular undersampling pattern leading to a discrete image domain aliasing pattern (or point spread function [PSF]), and is mostly intuitively implemented with integer undersample factors. For SMS imaging and its typically low number of k-space points along the slice direction, equivalent to the number of simultaneously excited slices, noninteger slice undersampling factors occur frequently. Note that a distinction needs to be made between *slice acceleration*, which is given by the number of simultaneously excited slices and thus determines the temporal speedup of the acquisition, and *slice undersampling* factor, which denotes the ratio between the sampled reduced FOV and the nominal full FOV (Nslices*slice gap) along the slice direction. For instance, $AF_z = 8$, CAIPI-3, corresponds to 8/3-fold slice undersampling because only three out of eight planes in k-space are sampled (see Figure 2). The k-space increment in slice direction (CAIPI blip moment) is then given as $\Delta k_{zR} = 2\frac{2}{3}\Delta k_z$, where Δk_z is the k-space increment that fulfills the Nyquist condition. This results in acquired samples that do not fall onto Cartesian grid points for a k-space with $N = 8$, as shown in Figure 2a. Slightly changing the applied k-space moment so that the acquired points lie on the grid destroys the periodic sampling pattern under circular shifts of k-space. By adding a "dummy slice" with zero intensity (Fig. 2b), we effectively increase the FOV in the slice direction and therefore decrease the k-space increment Δk_z^{ext} for full sampling. The k-space maximum, however, remains constant because it only depends on the slice separation d and is given as $k_{zmax} = k_{zmax}^{ext} = \frac{1}{2d}$. Because the number dummy slices was chosen to result in an integer slice acceleration factor, the acquired k-space points (identical to Fig. 2a) now fall onto the Cartesian grid for $N_{ext} = 9$ slices, and the problem becomes trivial to solve with SENSE. This approach of increasing the FOV by adding virtual slices in image space is called extended FOV reconstruction.

Similar in implementation, the extended FOV reconstruction must not be confused with conventional zero-padding of k-space in order to virtually increase the spatial resolution. In case of zero-padding, the k-space increment is maintained and k-space is extended beyond its original maximum, thereby increasing the apparent spatial resolution but keeping the FOV constant. In contrast, the extended FOV reconstruction changes the FOV and thereby the target k-space increment, whereas it maintains the k-space maximum and thereby the spatial resolution. The actual acquisition is not affected, and only the target k-space into which the acquired samples are sorted is adapted in order to achieve periodic k-space undersampling on a Cartesian grid.

An extended FOV reconstruction is only necessary in the context of a Cartesian SENSE type reconstruction that operates on periodic aliasing in the image domain. A non-Cartesian, iterative reconstruction approach (e.g., conjugate gradient-SENSE (16)) is able to directly reconstruct the acquired k-space pattern regardless of whether it is on a Cartesian grid or not. The latter is also true for GRAPP- type methods that operate directly in k-space such as the slice-GRAPPA.

METHODS

Image Acquisition

Experiments were performed on the Siemens 3T Tim Trio at the MR Research Center of the University of Hawaii and the Siemens Magnetom 7T scanner at Scannexus (www.scannexus.nl). Both scanners are equipped with 32-channel head receive arrays (3T: Siemens Healthcare, Erlangen, Germany; 7T: Nova Medical, Wilmington, MA). Data were acquired in $N = 4$ healthy subjects after obtaining informed consent under the institutionally approved protocols. Image reconstructions were performed offline using MATLAB (The MathWorks, Natick, MA).

Image Acquisition and Reconstruction

We show two examples of SMS reconstruction with SENSE. A single-shot blipped-CAIPI SMS-EPI acquisitions at 7T with matrix 96×96, 2.5-mm isotropic voxels,

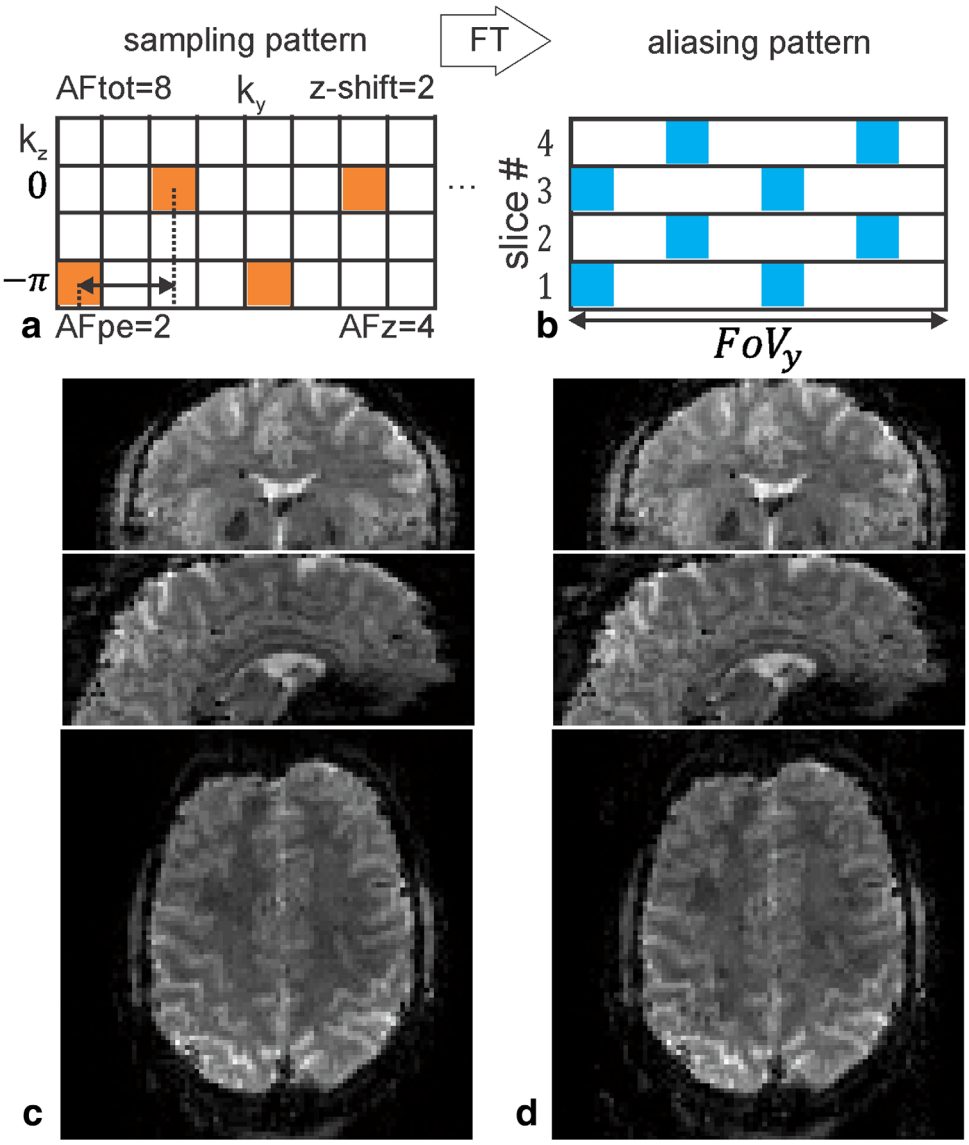

FIG. 1. Sampling pattern ($AF_{pe} = 2$, $AF_z = 4$, shift 2, matrix 96 × 96, 36 slices) displayed in (a) and 2D-SENSE aliasing pattern for SMS-EPI acquisition with in-plane undersampling. The grid size in slice direction is given by the slice acceleration factor of the multiband pulse (one SMS group). A total acceleration factor of eight results in eight nonzero PSF entries, as displayed in (b). Slice-GRAPPA and 2D-SENSE reconstructions are shown in (c) and (d), respectively.

36 slices in 9 SMS slice groups, $AF_z = 4$, $AF_{pe} = 2$, CAIPI-factor 2, slice separation $d = 20$ mm; and an SMS turbo spin echo (TSE)/RARE acquisition at 3T with PINS (power independent number of slices) multislice excitation (14) with matrix 256×256, 56 slices in 7 SMS-slice groups, $AF_z = 8$, $AF_{pe} = 1$, CAIPI-factor 3, slice-thickness 3 mm, SMS slice distance $d = 21$ mm, FOV = 250×250 mm, in-plane resolution 0.98 mm, bandwidth (BW) = 130Hz/pix that was acquired in 8 shots with echo train lengths = 32 (see (14) for further details).

To demonstrate the applicability of the reconstruction approach to volumetric as well as SMS acquisitions, two CAIPIRINHA 3D-EPI and blipped-CAIPI SMS-EPI datasets with corresponding geometry and undersampling parameters were acquired at 3T from the same subject in immediate succession. Identical acquisition parameters were used, and the k-space undersampling pattern was matched so that the total number of slices in case of the SMS-EPI acquisition was identical to the number of phase-encoding steps along the slice direction in case of 3D-EPI. The acquisitions thus employ exactly the same blipped EPI readout trajectory and differed only in slice phase encoding and slice selection. The imaging parameters were: matrix size 96×96, FOV = 25×250 mm^2, $2.3 \times 2.3 \times 3$ mm^3 voxels, 72 slices in 18 SMS slice groups (or 72 partitions acquired with 18 excitations in case of 3D-EPI), slice acceleration $AF_z = 4$, in-plane acceleration $AF_{pe} = 2$, CAIPI-factor 2, abd SMS slice separation $d = 41.5$ mm. For details on the CAIPIRINHA 3D implementation, see (10).

For all SENSE-based reconstructions, coil sensitivity maps were derived from fully sampled, short echo time-TR low-resolution gradient recalled echo scans covering the acquisition volume, subsequently dividing each coil by the sum-of-squares combination of all coil images and additional spatial smoothing with a $3 \times 3 \times 3$ Gaussian kernel.

For comparison, the 2D-SMS data were also reconstructed using the slice-GRAPPA method (2) with a 3×4 kernel, followed by a regular GRAPPA (17) reconstruction

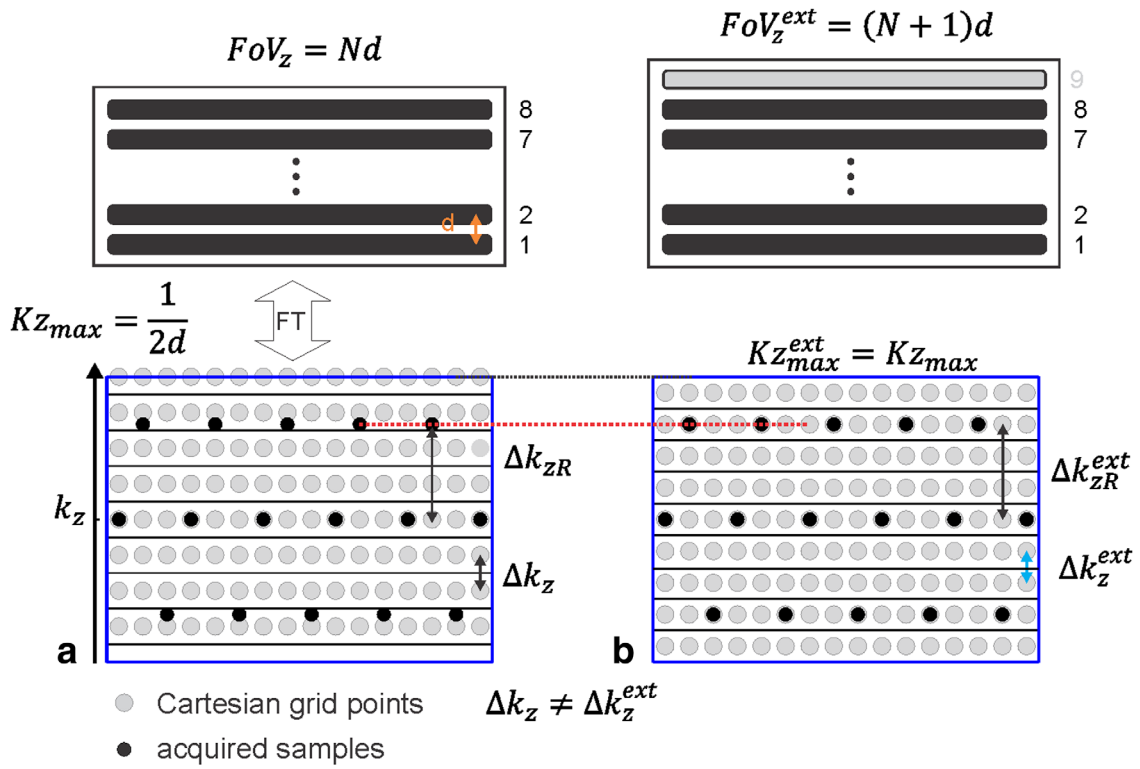

FIG. 2. Extended FOV reconstruction for noninteger slice undersampling. Adding a dummy slice in image space reduces the k-space increment so that the acquired samples fall onto the Cartesian grid. The dummy slices are removed in a postprocessing step.

with 3×4 kernel in case of additional in-plane undersampling.

RESULTS

SMS-EPI

Figure 1 shows the reconstruction of a 96×96 blipped-EPI reconstruction with two-fold in-plane undersampling ($AF_{pe} = 2$). The slice-GRAPPA reconstruction in the left column (c) and the SENSE reconstruction in the right column (d) result in images with minor differences. The two-fold in-plane undersampling results in an aliasing pattern with more than one nonzero entry per slice. The combined effect of in-plane and slice undersampling, however, does not result in a FOV/2 shift between neighboring slices. Only a shift by one-quarter of the FOV is present for neighboring slices. This observation does not affect the actual reconstruction for the slice-GRAPPA method or the SENSE approach. However, it provides an instructive illustration that the reconstruction problem is best described with two dimensions, assuming that the read direction is fully sampled.

SMS-RARE

Figure 3 shows the extended FOV SENSE reconstruction of the RARE (13) data. The sampling pattern and the aliased PSF are shown in Figure 3a and 3b. The dummy slices, added to facilitate integer SENSE reconstruction, and the resulting virtual entry in the aliasing pattern are indicated in gray. In Figure 3c, one reconstructed SMS group (sagittal orientation) is shown, including the dummy slice that is reconstructed as a regular slice with zero intensity. The dummy slices are then removed in a postprocessing step. Figure 3d displays the reconstructed volume as three orthogonal slices.

Common Reconstruction Pipeline for 3D- and SMS-EPI

Figure 4 demonstrates the ability of the SENSE approach to reconstruct 3D datasets either acquired with conventional slab or SMS excitation. In Figure 4a, the k-space sampling patterns for both imaging modalities are shown (orange for SMS-EPI and blue for 3D-EPI). Because the acceleration parameters are identical in both cases ($AF_z = 4$, $AF_{pe} = 2$, CAIPI-shifts 2) the 3D k-space for the scan with volume excitation and partition encoding can be obtained by stacking replicas of the SMS k-space (depicted with gray background) 18 times. The effective volume TR is consequently the same for both scans ($TR_{vol} = 600$ ms; $18 \times$ the slice excitation TR, which was TR = 50 ms). Exactly the same reconstruction pipeline and coil sensitivity estimation was used for both acquisitions, with the obvious exception of the k-space dimension along the slice direction (4 in case of SMS-EPI; 72 in case of 3D-EPI). The corresponding reconstructions are shown in Figure 4b for the SMS-EPI scan and in Figure 4c for the 3D-EPI scan. The expected contrast difference between the 2D- and 3D-EPI scans naturally results from the difference in tissue excitation rate (600 ms vs. 50 ms). The identical volume TR, however, makes them directly comparable choices for functional MRI use. The SENSE reconstruction approach performs equally well for 3D and SMS data with no visible artifacts due to the

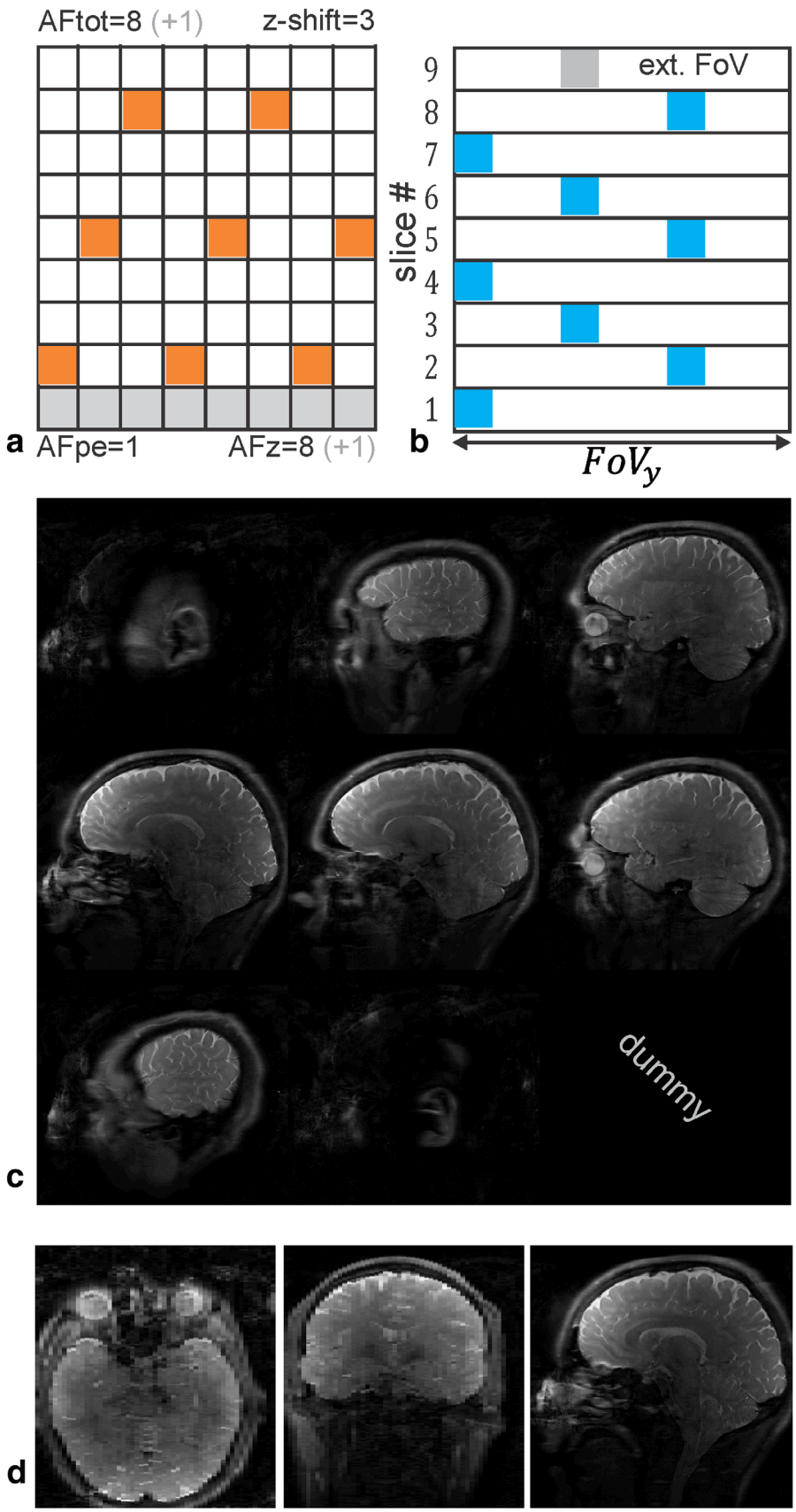

FIG. 3. Reconstruction of a PINS-RARE dataset with dummy slices. The extended FOV undersampling and aliasing patterns for AFpe = 1, AFz = 8, and CAIPI-3 are shown in (a) and (b), respectively. One SMS group reconstructed with 2D-SENSE, including the additional dummy slice, is shown in (c). Three orthogonal slices out of the full volume are shown in (d).

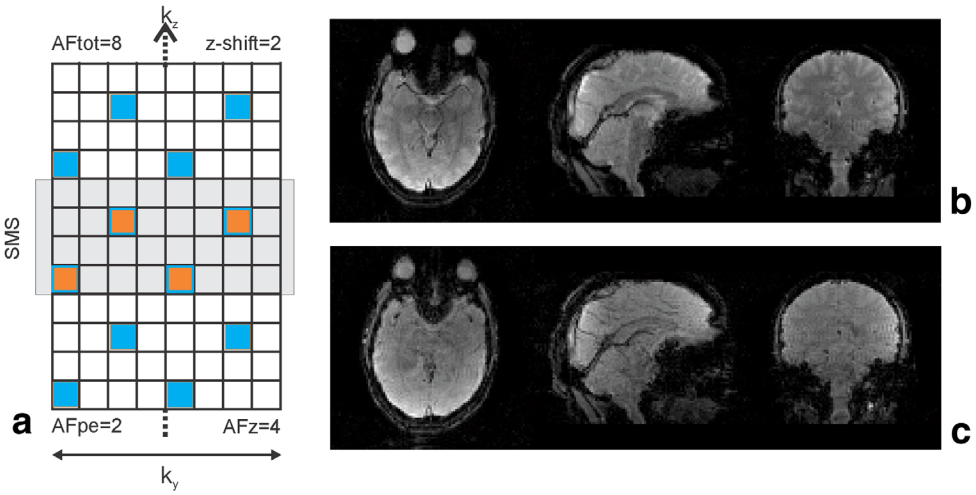

FIG. 4. Common reconstruction pipeline for SMS-EPI and volumetric 3D-EPI acquisitions. In (a), the sampling pattern for SMS-EPI is depicted with orange squares. Because both acquisition modalities use identical undersampling parameters ($AF_z = 4$, $AF_{pe} = 2$, CAIPI-shifts 2), the pattern for 3D-EPI (blue squares) can be generated by replicating the SMS-EPI pattern along the slice phase-encoding dimension. In (b) and (c), the reconstructed volumes are shown for SMS-EPI and 3D-EPI, respectively.

slice or in-plane acceleration. Also, because both methods share the same coil sensitivity data (derived from a short TR prescan) and undersampling pattern, the pixel locations that fold onto each other are also identical; therefore, each subproblem of the SENSE algorithm has identical coil sensitivity weighting coefficients. Because the g-factor penalty g_p only depends on the coil sensitivity weighting coefficients S and potential noise-correlations between the coils Ψ by $g_p = \sqrt{\left(S^H\Psi^{-1}S\right)^{-1}_{pp}\left(S^H\Psi^{-1}S\right)_{pp}}$ (see ref. (8)), it is also identical for both modalities. Any observable difference in SNR or temporal SNR between 2D- and 3D-EPI can thus be attributed to sequence specific contributions such as 2D- versus 3D-excitation, in-flow effects, and effective TR difference.

DISCUSSION

The present work demonstrates that a 2D-SENSE approach can be used for a wide variety of reconstructions with optimized k-space undersampling patterns for both volumetric and SMS excitation (i.e., blipped-CAIPI EPI, PINS-TSE, and 3D-EPI with volumetric CAIPIRINHA). A 2D-SENSE approach is conceptually simple and easy to implement. In case of additional in-plane undersampling, it provides a one-step reconstruction along both undersampled dimensions, which may be potentially more stable numerically than a two-step approach. It also provides a contrast-independent parallel imaging reconstruction by using actual coil sensitivity maps instead of relying on a training dataset.

The aim of this paper has not been to perform a direct comparison of SNR or other reconstruction properties of SENSE with other methods such as slice-GRAPPA. Well-tuned reconstructions of both types can be expected to deliver images of very comparable image quality. As in other GRAPPA-type reconstructions, the g-noise distribution (18) in a two-step slice-GRAPPA/GRAPPA reconstruction may be smoother than in a SENSE reconstruction but with comparable values. GRAPPA reconstruction may be less sensitive to imperfections in the reference data because the inverse problem is highly overdetermined, whereas a good SENSE reconstruction stands and falls with the quality of the sensitivity map. A conceptual advantage of SENSE type approaches is the contrast independence between the sensitivity maps and the undersampled data, which may lead to improved reconstructions for highly diffusion-weighted, perfusion-weighted, or angiographic acquisitions whose contrast spatial frequency spectrum differs significantly from typical calibration data with flat contrast. Another method that deals with the contrast problem is given by the so-called split slice-GRAPPA (19) approach, which is based on optimized kernels. One practical advantage of SENSE reconstructions is that they are highly parallelizable on graphics processing-units (GPU) hardware with minimal working memory requirements because each set of aliased voxels can be reconstructed completely independently of the rest. We also demonstrated that by using 2D-SENSE, a single reconstruction pipeline can be used to reconstruct volumetric (i.e., 3D-EPI) and SMS data (i.e., blipped-EPI). For the ongoing debate over the advantages/disadvantages of segmented volumetric EPI versus 2D single-shot EPI, this might prove very helpful to perform a fair comparison in terms of temporal SNR without introducing any bias from a sequence specific reconstruction method. Because g-noise will be the same in both 2D-SMS and 3D-reconstructions, any observed differences can unequivocally be attributed to differences in the imaging experiment itself, such as (functional) imaging contrast and sensitivity or differing contributions of physiological fluctuations.

CONCLUSION

A straightforward 2D-SENSE implementation can be used to reconstruct SMS excitations with arbitrary blipped CAIPIRINHA undersampling patterns. One reconstruction pipeline can be used for SMS and volumetric imaging.

REFERENCES

1. Moeller S, Yacoub E, Olman CA, Auerbach E, Strupp J, Harel N, Ugurbil K. Multiband multislice GE-EPI at 7 Tesla, with 16-fold acceleration using partial parallel imaging with application to high

spatial and temporal whole-brain fMRI. Magn Reson Med 2010;63: 1144–1153.
2. Setsompop K, Gagoski BA, Polimeni JR, Witzel T, Wedeen VJ, Wald LL. Blipped-controlled aliasing in parallel imaging for simultaneous multislice echo planar imaging with reduced g-factor penalty. Magn Reson Med 2012;67:1210–1224.
3. Breuer FA, Blaimer M, Heidemann RM, Mueller MF, Griswold MA, Jakob PM. Controlled aliasing in parallel imaging results in higher acceleration (CAIPIRINHA) for multi-slice imaging. Magn Reson Med 2005;53:684–691.
4. Breuer FA, Blaimer M, Mueller MF, Seiberlich N, Heidemann RM, Griswold MA, Jakob PM. Controlled aliasing in volumetric parallel imaging (2D CAIPIRINHA). Magn Reson Med 2006;55:549–556.
5. Zhu K, Kerr A, Pauly JM. Autocalibrating CAIPIRINHA: Reformulating CAIPIRINHA as a 3d problem. In Proceedings of the 20th Annual Meeting of the ISMRM, Melbourne, Australia. 2012. p. 518.
6. Breuer F, Blaimer M, Seiberlich N, Griswold MA, Jakob PM. A 3D GRAPPA algorithm for volumetric parallel imaging. In Proceedings of the 14th Annual Meeting of ISMRM, Seattle, Washington, USA, 2006. p. 286.
7. Stab D, Ritter CO, Breuer FA, Weng AM, Hahn D, Kostler H. CAIPIRINHA accelerated SSFP imaging. Magn Reson Med 2011;65:157–164.
8. Pruessmann KP, Weiger M, Scheidegger MB, Boesiger P. SENSE: Sensitivity encoding for fast MRI. Magn Reson Med 1999;42:952–962.
9. Weiger M, Pruessmann KP, Boesiger P. 2D SENSE for faster 3D MRI. MAGMA 2002;14:10–19.
10. Poser BA, Kemper VG, Ivanov D, Uludag K, Kannengiesser SA, Barth M. Caipirinha-accelerated 3d epi for high temporal and/or spatial resolution EPI acquisitions. In Proceedings to ESMRMB Congress, Toulouse, France; 2013. p. 287.
11. Narsude M, Gallichan D, Gruetter R. Superior grappa reconstruction with reduced g-factor noise using 2d CAIPIRINHA for 3d EPI. 2013; Melbourne, Australia. p. 3705.
12. van der Zwaag W, Marques JP, Kober T, Glover G, Gruetter R, Krueger G. Temporal SNR characteristics in segmented 3D-EPI at 7T. Magn Reson Med 2012;67:344–352.
13. Hennig J, Nauerth A, Friedburg H. RARE imaging: a fast imaging method for clinical MR. Magn Reson Med 1986;3:823–833.
14. Norris DG, Boyacioglu R, Schulz J, Barth M, Koopmans PJ. Application of PINS radiofrequency pulses to reduce power deposition in RARE/turbo spin echo imaging of the human head. Magn Reson Med 2014;71:44–49.
15. Zahneisen B, Poser BA, Ernst T, Stenger VA. Three-dimensional Fourier encoding of simultaneously excited slices: generalized acquisition and reconstruction framework. Magn Reson Med 2014;71: 2071–2081.
16. Pruessmann KP, Weiger M, Bornert P, Boesiger P. Advances in sensitivity encoding with arbitrary k-space trajectories. Magn Reson Med 2001;46:638–651.
17. Griswold MA, Jakob PM, Heidemann RM, Nittka M, Jellus V, Wang JM, Kiefer B, Haase A. Generalized Autocalibrating Partially Parallel Acquisitions (GRAPPA). Magn Reson Med 2002;47:1202–1210.
18. Breuer FA, Kannengiesser SA, Blaimer M, Seiberlich N, Jakob PM, Griswold MA. General formulation for quantitative G-factor calculation in GRAPPA reconstructions. Magn Reson Med 2009;62: 739–746.
19. Cauley SF, Polimeni JR, Bhat H, Wald LL, Setsompop K. Interslice leakage artifact reduction technique for simultaneous multislice acquisitions. Magn Reson Med 2014;72:93–102.